JACS
JOURNAL OF THE AMERICAN CHEMICAL SOCIETY
pubs.acs.org/JACS

Open Access
This article is licensed under CC-BY-NC-ND 4.0

Article

Bioorthogonal Photocatalytic Protein Labeling and Cross-Linking Enabled by Stabilized Ketyl Radicals

Jiawei Tan,[#] Kejia Hao,[#] Yi Yuan,[#] Shasha Xie,[#] Li Qi,[#] Qiaoling Che,[#] Yan Li, Renxiao Wang,* Yaoyang Zhang,* and Yiyun Chen*

Cite This: J. Am. Chem. Soc. 2025, 147, 45774−45784

Read Online

ACCESS | Metrics & More | Article Recommendations | Supporting Information

ABSTRACT: Radical reactions offer transformative potential in biological contexts but remain constrained by poor selectivity and off-target reactivity. We address these limitations through visible-light photocatalytic generation of diaryl ketyl radicals from benzophenones. This strategy circumvents traditional UV excitation pathways by suppressing triplet diradical formation—which drives nonspecific [2 + 2] cycloadditions and H atom abstraction—in favor of bioorthogonal radical−radical coupling. Our platform enables precise live-cell protein labeling with minimal cytotoxicity, including in sensitive primary neuronal cultures, and achieves site-specific modification via genetically incorporated benzophenone-based unnatural amino acids Bpa. The spatial selectivity of this approach exceeds conventional UV-based cross-linking methods, facilitating site-to-site analysis of tertiary protein interactions in structurally defined complexes. We demonstrate these capabilities by (1) quantifying dimerization interfaces of the Diels−Alderase PyrI4 and (2) resolving Bcl-X_L/Bid interactions critical for apoptotic regulation. This photocatalysis-driven methodology establishes a robust alternative to cycloaddition-based bioorthogonal chemistry for spatiotemporally controlled interrogation of dynamic biomolecular processes.

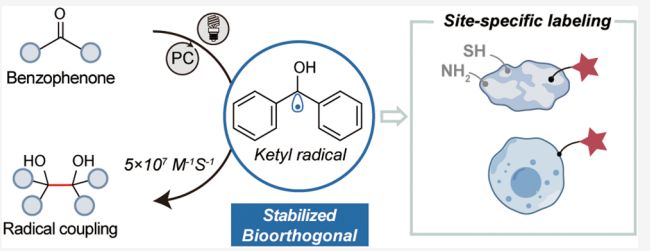

Downloaded via 91.199.84.137 on December 12, 2025 at 07:01:07 (UTC).
See https://pubs.acs.org/sharingguidelines for options on how to legitimately share published articles.

INTRODUCTION

Radical reactions offer exceptional versatility in organic synthesis,[1] and may hold significant promise for biological applications due to their single-electron mechanisms and aqueous compatibility.[2] Advances in photoredox catalysis have enabled mild,[3] selective radical generation under biocompatible conditions,[2b,4] driving innovations in posttranslational mutagenesis and enzymatic synthesis.[5] However, the inherent reactivity of radical intermediates often causes off-target reactions in biological environments. Conventional strategies—including radical additions[6]—employ highly reactive species that nonspecifically modify native protein residues (Figure 1A), limiting their utility in complex systems.[7] Similarly, benzophenone photochemistry relies on direct UV excitation to generate triplet diradicals for bioconjugation.[8] Yet this approach lacks bioorthogonality due to indiscriminate [2 + 2] cycloadditions and H atom abstraction (HAT) with endogenous biomolecules, invariably causing off-target modifications.

In contrast, radical−radical coupling leverages stabilized radical species to minimize off-target reactivity,[2b,9] aligning with bioorthogonal principles for precise biomolecular engineering.[10] Here, we introduce a photocatalytic strategy using visible light to generate stabilized diaryl ketyl radicals from benzophenones. This mechanism bypasses triplet diradical formation (Figure 1B), exploiting steric and resonance effects to extend radical lifetimes[11] while avoiding traditional HAT/[2 + 2] side reactions. Critically, these ketyl radicals[12] undergo ultrafast homocoupling ($k = 5.9 \times 10^7$ M^{-1} s^{-1}) that outcompetes biomolecular quenching pathways, enabling bioorthogonal protein modification and cross-linking with minimal off-target reactivity (Figure 1C).[13]

RESULTS AND DISCUSSION

Discovery of Bioorthogonal Ketyl Radical Coupling in Aqueous Media. Translating diaryl ketyl radical−radical coupling from organic solvents[14] to bioorthogonal applications in cellular environments faces inherent challenge[15] due to radical quenching by biomolecules, pH variations, and ionic strength.[16] To establish an optimal system for biological application, we systematically screened photocatalysts and reductants under blue LED irradiation in aqueous buffer (pH 7.4). The $Ru(bpy)_3Cl_2$/ascorbic acid (VcH) pair emerged as optimal, achieving a 92% yield of pinacol **2** from benzophenone **1** (Figure 2A). While several Ru(II) polypyridyl complexes achieved high yields, the performance of Ir(III) photosensitizers was significantly lower (e.g., 17% yield after 10

Received: October 22, 2025
Revised: November 11, 2025
Accepted: November 13, 2025
Published: November 28, 2025



© 2025 The Authors. Published by American Chemical Society

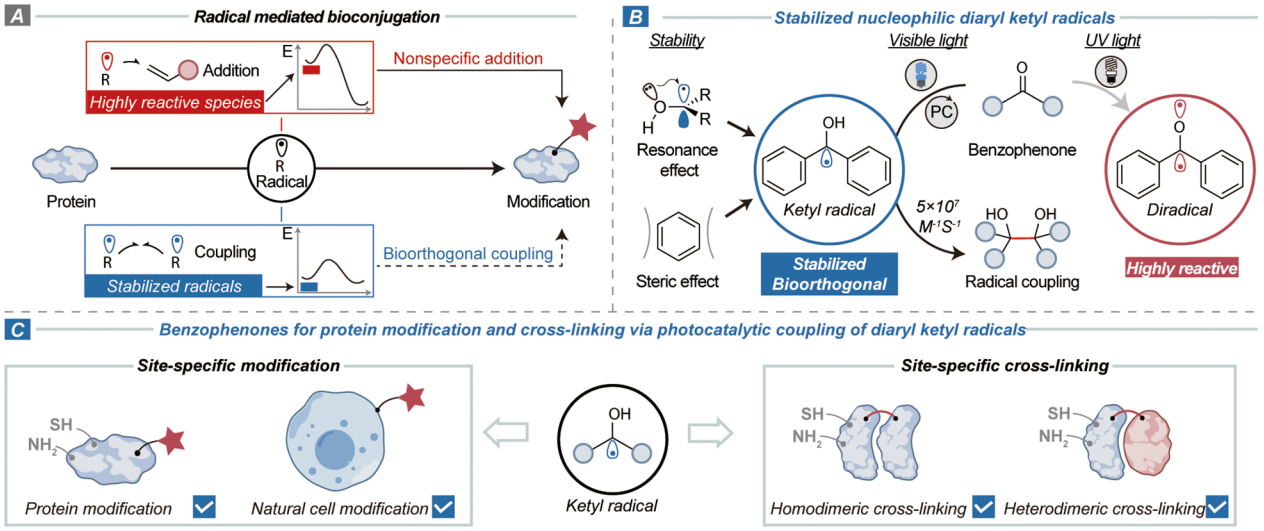

Figure 1. Bioorthogonal protein labeling via photocatalytic ketyl radicals. (A) Conventional methods use highly reactive radicals causing nonspecific modifications (top) versus our stabilized ketyl radicals enabling selective bioorthogonal coupling (bottom). (B) UV photoexcitation generates reactive triplet diradicals that undergo uncontrolled H-abstraction/[2 + 2] cycloadditions (red). Visible-light photocatalysis produces stabilized diaryl ketyl radicals via steric/resonance effects, directing selective radical−radical coupling (blue). (C) Benzophenone-functionalized proteins undergo site-specific labeling and cross-linking through photocatalytic ketyl radical homocoupling.

min, only rising to 89% after 10 h). This disparity is attributed to an optimal reduction potential window—catalysts with excessively negative potentials (e.g., *fac*-Ir(ppy)$_3$, E_p = −2.19 V) were ineffective—and the superior aqueous compatibility of Ru(II) complexes, which sustained high efficacy in physiological media unlike their Ir(III) counterparts (Figure S1, Table S1).

Reductant screening revealed VcH as uniquely effective, a property not fully explained by superior photocatalyst quenching alone. Although VcH exhibited only a 1.7-fold higher quenching constant than DIPEA for [Ru(bpy)$_3^{2+}$]*, the benzophenone-VcH complex showed a 2.3-fold higher quenching constant (Figure S2), indicating synergistic preassociation.[17] NMR titration confirmed this interaction through chemical shift changes consistent with hydrogen bonding, while DOSY NMR verified formation of a distinct molecular complex (Figure S4−S5). This preactivation mechanism dramatically lowers the reduction barrier of benzophenone (Figure S3).[18] Furthermore, UV−vis absorption studies excluded a potential EDA complex pathway, and higher triplet energy of benzophenone (69.1 kcal/mol) compared to Ru(II)[19] ruled out energy transfer mechanisms (Figure S12). Thus, the Ru(bpy)$_3$Cl$_2$/VcH pair is uniquely effective because it synergistically integrates optimal reducing power and aqueous solubility (Ru catalyst) with substrate preactivation that lowers the kinetic barrier (VcH).

The system exhibits exceptional functional group orthogonality, tolerating amino acids, nucleosides, and carbohydrates (Table S5). Benzophenone **1** and pinacol **2** display superior stability to common bioorthogonal reagents (e.g., tetrazines **3**/cyclooctynes **4**[20]), resisting glutathione, oxidative/acidic/alkaline conditions (Figure S9, S10). Radical trapping with 4-cyanopyridine verified ketyl radical intermediacy by photocatalytic conditions (Figure 2B). Crucially, photocatalytic ketyl radicals exhibit distinct reactivity from UV-excited benzophenone triplet diradicals. Three independent lines of evidence rule out triplet-state involvement: (1) They showed no consumption of amino acids or olefin triplet acceptors (e.g., vinyl ether or dThd), confirming the absence of nonspecific reactions characteristic of triplet states (Figure 2C, Figure S13).[21] (2) The photocatalytic system resulted in minimal uric acid and ADPA consumption (<5%), indicating no detectable singlet oxygen ($^1O_2$) production and, by extension, no triplet-energy transfer pathway (Figure S14−S15).[22] (3) Most tellingly, while O_2 purging suppressed initial conversion rates—consistent with radical quenching—prolonged irradiation under O_2 still achieved standard yields. This oxygen compatibility, demonstrating efficient ketyl radical regeneration within the cycle, is inconsistent with the irreversible quenching of a long-lived triplet state (Table S6). Collectively, these three orthogonal lines of evidence definitively rule out the involvement of a traditional benzophenone triplet diradical mechanism, establishing the distinct nature of the photocatalytic ketyl radical pathway. This bioorthogonality, combined with rapid kinetics and substrate stability, overcomes the stability-reactivity trade-off inherent to cycloaddition-based methods, establishing a versatile platform for aqueous biomolecular engineering (Figures S16−S19).

Site-Specific Labeling of Proteins via Photocatalytic Ketyl Radical Coupling. To demonstrate the applicability of this reaction for protein labeling, we modified Bcl-X_L with SulfoNHS-BP **5** containing benzophenone groups.[15] Additionally, we have designed and synthesized a protein labeling probe, Biotin-BP **6**, comprising a biotin reporter group and a benzophenone moiety (Figure 3A). Subsequently, we incubated the modified Bcl-X_L protein with a reaction mixture containing Ru(bpy)$_3$Cl$_2$, VcH, and Biotin-BP **6**. Upon blue light irradiation, Western blot analysis revealed efficient labeling of the benzophenone-modified Bcl-X_L with Biotin-BP **6**. In contrast, the unmodified Bcl-X_L showed no labeling, confirming the specificity of the reaction (Figure 3B). The LC-MS results revealed that the photolabeling signal of Bcl-X_L originated specifically from lysine modifications and exactly coincided with the benzophenone-labeled sites (Figure S20). This demonstrates that the reaction is highly specific to the preinstalled benzophenone handles. The observed selectivity for a subset of lysine residues—a pattern that is generalizable across different proteins like BSA (Figure S21)—is a

https://doi.org/10.1021/jacs.5c18652
J. Am. Chem. Soc. 2025, 147, 45774−45784

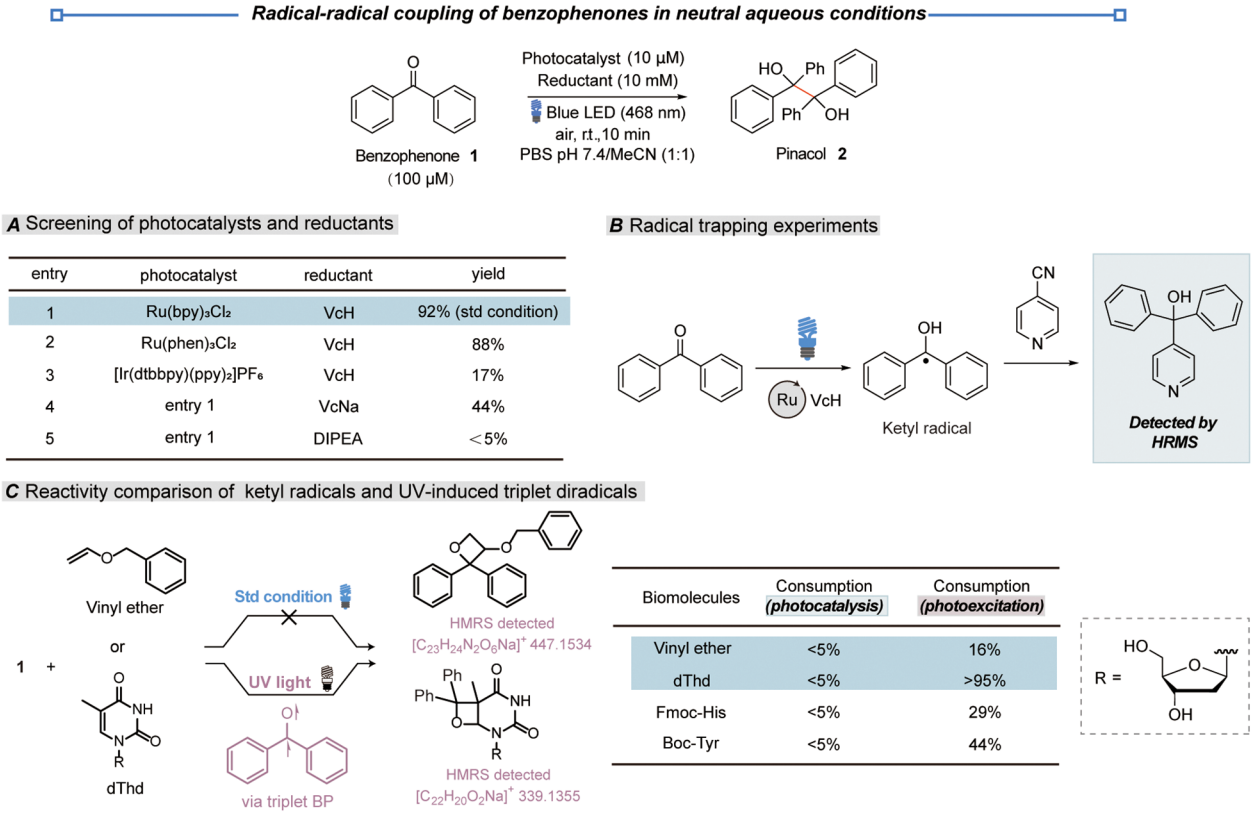

Figure 2. Bioorthogonal ketyl radical coupling in aqueous media. (A) Screening of photocatalyst (10 μM) and reductant (10 mM). Yields were determined by HPLC quantification. Standard (std) conditions: 100 μM benzophenone **1**, 10 μM $Ru(bpy)_3Cl_2$, 10 mM VcH, 468 nm light irradiation (4.5 mW/cm^2) for 10 min in PBS pH 7.4/MeCN (1:1). (B) Radical trapping experiments. Benzophenone **1** (0.1 mmol), VcH (0.15 mmol), $Ru(bpy)_3Cl_2$ (0.002 mmol), and 4-cyanopyridine (0.3 mmol) in pH 7.4 buffered PBS/MeCN (1:1) under 468 nm light irradiation (20 mW/cm^2) for 12 h under a nitrogen atmosphere at room temperature. (C) Reactivity comparison: photocatalytic ketyl radicals versus UV-induced triplet diradicals. Left: HRMS detection confirms the formation of signature [2 + 2] cycloaddition products from reactions between benzophenone (1 mM) and dThd or vinyl ether (1 mM) under UV light (365 nm). Right: Quantitative comparison of alkene consumption. HPLC analysis shows >95% of alkene substrates remain unreacted under photocatalytic conditions (468 nm) versus significant consumption under UV photoexcitation (365 nm), demonstrating high selectivity. Reaction conditions: Photocatalysis: Benzophenone (1 mM), VcH (10 mM), $Ru(bpy)_3Cl_2$ (10 μM) in MeCN/PBS (pH 7.4, 1:1 v/v), 468 nm light (4.5 mW/cm^2, 10 min). Photoexcitation: Benzophenone (1 mM) with alkene substrates in MeCN/PBS, 365 nm UV light (0.2 mW/cm^2, 10 min).

predictable outcome of the NHS-ester chemistry, which modifies only solvent-accessible lysines as governed by the protein's tertiary structure.

We then modified the HeLa cell surface with benzophenone groups using SulfoNHS-benzophenone **5**, a cell-impermeable NHS ester that reacts with lysines of membrane proteins. Subsequently, cells were incubated with a reaction mixture containing Biotin-BP **6**, $Ru(bpy)_3Cl_2$, and VcH. Following blue light irradiation, confocal microscopy revealed efficient labeling of benzophenone-modified HeLa cells, with a significant increase in biotinylated signals localized at the cell surface (Figure 3C). Control experiments confirmed the specificity of the labeling. Flow cytometry analysis further supported these findings, demonstrating selective labeling of benzophenone-modified cells with Biotin-BP **6** (Figure 3C). To evaluate biocompatibility, we conducted MTT cell viability assays in HeLa and HEK293T cells following photocatalytic labeling. No significant cytotoxicity was observed (Figure S23−S24), confirming the excellent biocompatibility of our photocatalytic method. Based on these experiments, the reaction demonstrates high efficiency and significant potential for modifying live-cell systems. We quantitatively addressed the potential formation and impact of homodimers (e.g., of compound **6**), a concern for bioorthogonal efficiency. HPLC analysis of the reaction supernatant from live cells revealed a homodimer yield of 35% under standard photocatalytic conditions (Figure S25A). This confirms that while homodimerization occurs, the desired cross-coupling reaction with the target protein effectively outcompetes it. Crucially, the homodimer itself does not interfere with the labeling strategy: it exhibits excellent photostability (>95% remaining after 2 h irradiation) and, when added exogenously, has a negligible impact (<2%) on the target reaction yield (Figure S25B). Furthermore, the homodimer shows no cytotoxicity (IC_{50} > 200 μM) and generates no background signal in cells, confirming its biological inertness (Figure S25C). These results demonstrate that homodimer formation is a manageable side reaction that does not compromise the efficiency or interpretation of our photocatalytic labeling.

The nervous system is a highly intricate network of neurons connected by nanoscale synapses.[23] Bioorthogonal chemistry-mediated protein labeling has emerged as a valuable tool for investigating the dynamic changes in neuron-specific receptors.[24] However, current bioorthogonal techniques often lack the necessary spatiotemporal resolution to capture rapid neuronal events. Light-induced reactions, such as photo-

https://doi.org/10.1021/jacs.5c18652
J. Am. Chem. Soc. 2025, 147, 45774−45784

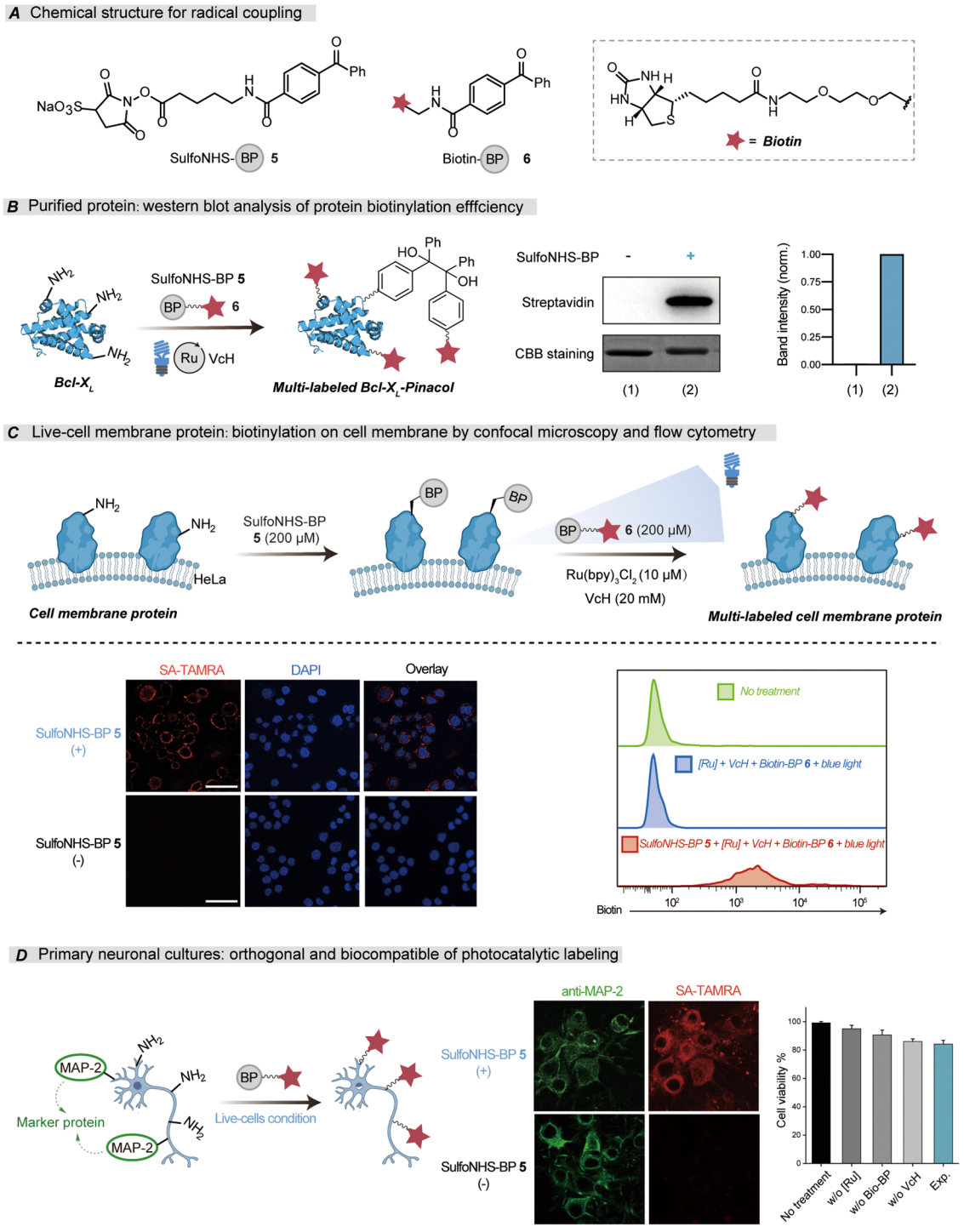

Figure 3. Site-specific labeling of proteins via photocatalytic ketyl radical coupling. (A) Schematic illustration and chemical structures of the benzophenone-based probes (e.g., Biotin-BP **6**) used for photocatalytic radical−radical coupling. (B) Analysis of protein biotinylation efficiency. Western blot analysis confirms successful photocatalytic biotinylation of Bcl-X_L protein. Comparison of reactions with and without the benzophenone precursor (SulfoNHS-BP **5**) demonstrates target-specific labeling. Reaction conditions: Bcl-X_L (10 μM), SulfoNHS-BP **5** (100 μM), $Ru(bpy)_3Cl_2$ (10 μM), VcH (20 mM), Biotin-BP **6** (100 μM) in PBS (pH 7.4), irradiated with 468 nm light (8.2 mW/cm^2, 10 min). (C) Live-cell membrane labeling. Confocal microscopy and flow cytometry analysis of HeLa cells show efficient cell-surface biotinylation dependent on photocatalytic labeling. Procedure: Cells were incubated with SulfoNHS-BP **5** (200 μM, 37 °C, 30 min), followed by treatment with $Ru(bpy)_3Cl_2$ (10 μM), VcH (20 mM), and Biotin-BP **6** (200 μM) in PBS and irradiation with 468 nm light (14.4 mW/cm^2, 15 min, RT). Cells were then fixed and stained with streptavidin-TAMRA (imaging) or streptavidin-Cy5 (flow cytometry). Scale bar: 50 μm. (D) Orthogonality and biocompatibility of photocatalytic labeling in primary neurons. Left: Schematic of the labeling strategy. Middle: Confocal microscopy shows specific biotinylation (red) colocalized with neuronal markers (green), demonstrating precise targeting. Right: Quantitative MTT assay reveals high cell viability (>84%) under standard conditions.

https://doi.org/10.1021/jacs.5c18652
J. Am. Chem. Soc. 2025, 147, 45774−45784

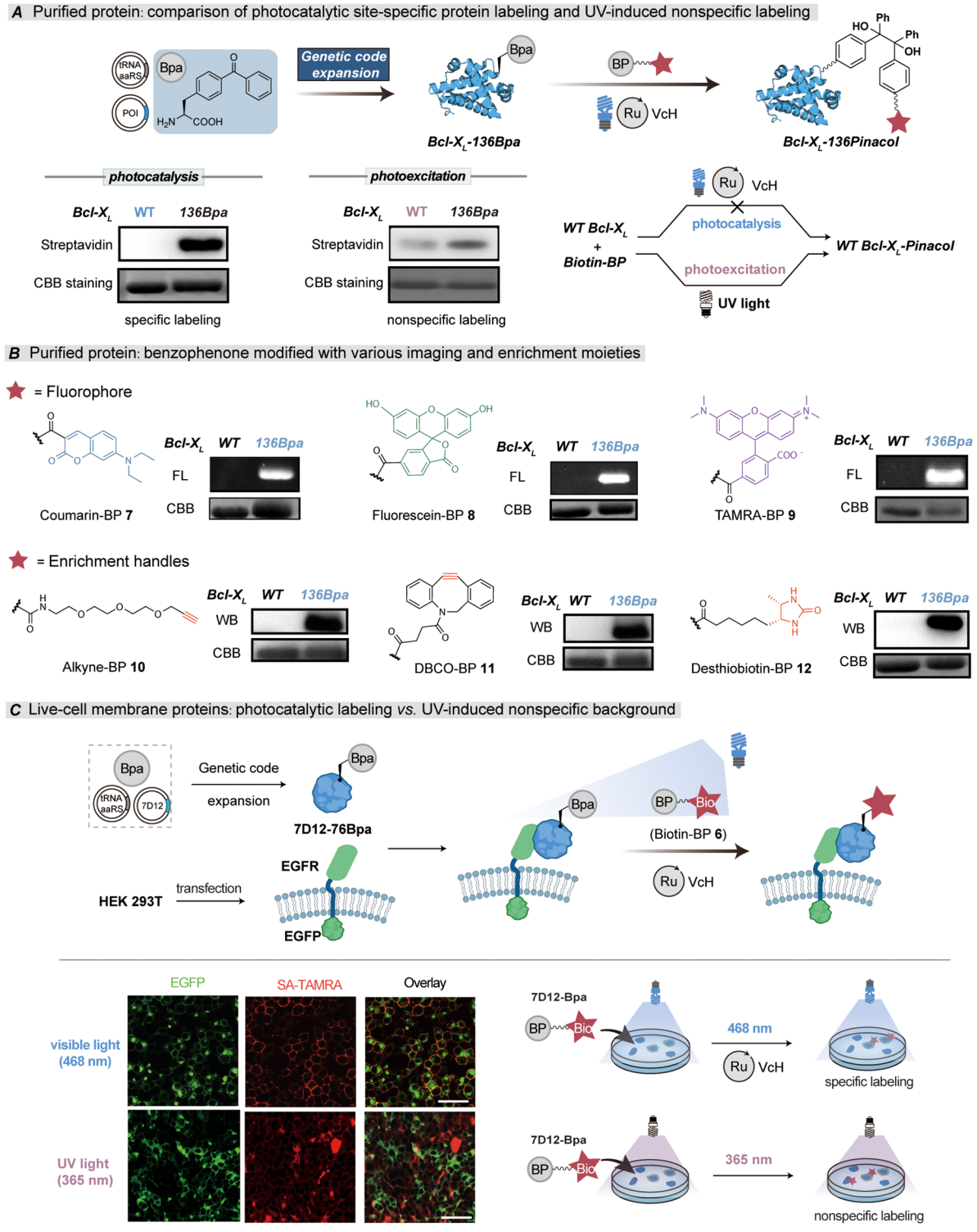

Figure 4. Photocatalytic benzophenone coupling for site-specific protein modification by genetic code engineering with unnatural amino acid Bpa. (A) Comparison of photocatalytic site-specific protein labeling and UV-induced nonspecific labeling. Proteins (Bcl-X_L-136Bpa/WT Bcl-X_L) were incubated and irradiated under two conditions: Photocatalytic group: 468 nm light (4.5 mW/cm^2, 10 min) with the addition of 100 μM Biotin-BP VcH (20 mM) and $Ru(bpy)_3Cl_2$ (10 μM); UV photoexcitation group: 365 nm UV light (0.2 mW/cm^2, 10 min) directly with the addition of 100 μM Biotin-BP. (B) Benzophenone modified with various imaging and enrichment moieties using in-gel fluorescence and Western blot separately. Reaction conditions: 10 μM Bcl-X_L-136Bpa, 10 μM $Ru(bpy)_3Cl_2$, 20 mM VcH, and 100 μM moieties **7**−**12** in PBS (pH 7.4) irradiated with 468 nm blue light (8.2 mW/cm^2) at room temperature for 10 min. (C) Photocatalytic labeling demonstrates specific membrane targeting versus UV-induced nonspecific background. Top: Schematic of the labeling strategy: EGFR-EGFP-expressing 293T cells were treated with the nanobody 7D12−76Bpa and subsequently labeled with Biotin-BP **6** under uniform illumination. Middle: Photocatalytic labeling (468 nm) shows specific colocalization of EGFP (green, target) and SA-TAMRA (red, label) signals after fixation and staining, demonstrating precise membrane targeting. Bottom: Photolytic labeling (365 nm) results in widespread nonspecific background labeling without target colocalization, highlighting the superior specificity of the photocatalytic approach.

https://doi.org/10.1021/jacs.5c18652
J. Am. Chem. Soc. 2025, 147, 45774−45784

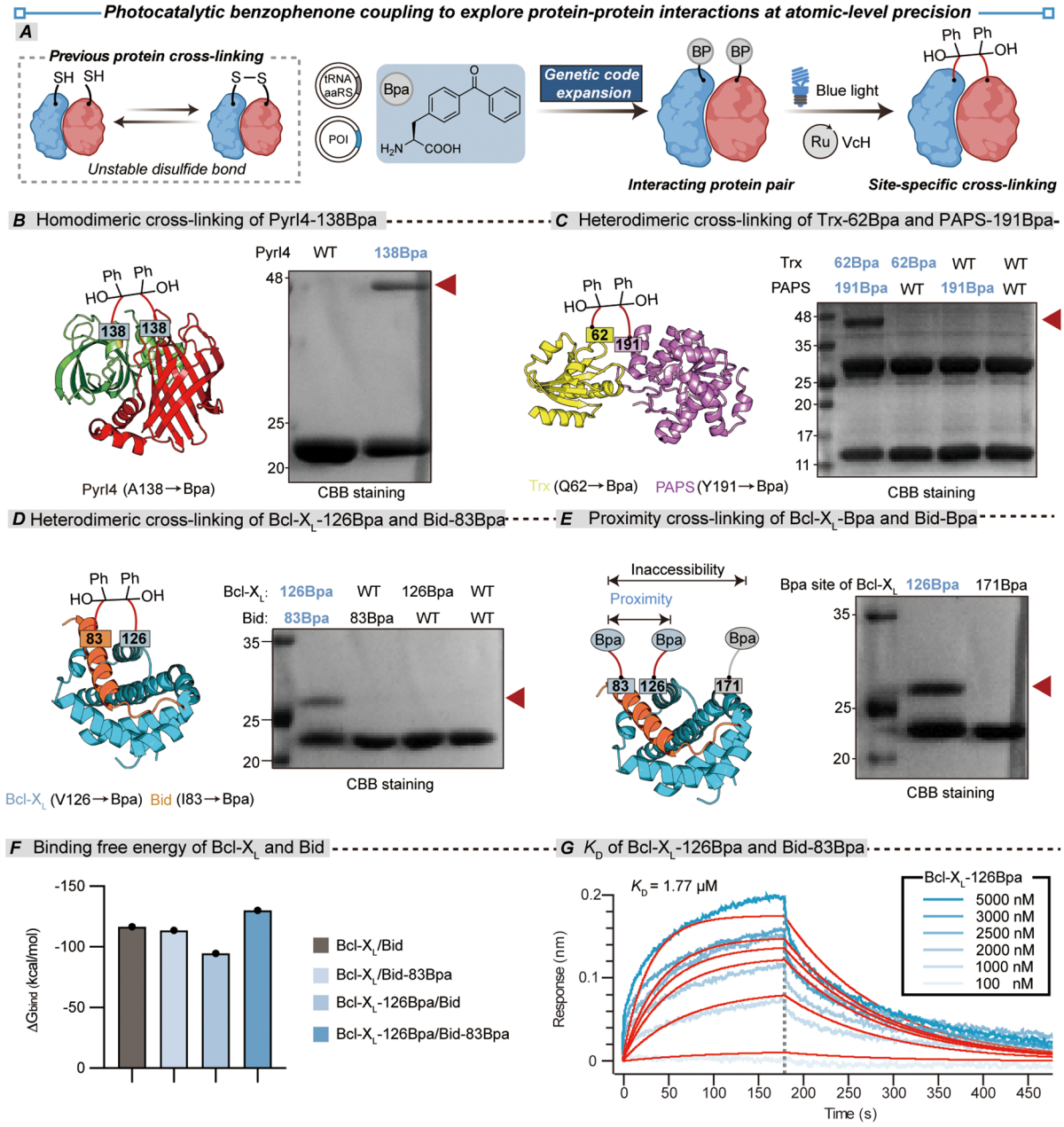

Figure 5. Photocatalytic benzophenone coupling to explore protein−protein interactions at atomic-level precision. (A) Schematic illustration of protein−protein cross-linking. Reaction conditions: 10 μM genetically encoded protein with Bpa, 10 μM $Ru(bpy)_3Cl_2$, 20 mM VcH, 468 nm light irradiation in PBS buffer (pH 7.4) for 10 min. (B) Homodimeric cross-linking of PyrI4−138Bpa. (C) Heterodimeric cross-linking of Trx-62Bpa and PAPS-191Bpa. (D) Heterodimeric cross-linking of Bcl-X_L-126Bpa and Bid-83Bpa. (E) Proximity cross-linking of Bid-83Bpa Bcl-X_L-126Bpa/171Bpa. (F) Binding free energy of Bcl-X_L and Bid by molecular dynamics simulation. (G) K_D of Bcl-X_L-126Bpa and Bid-83Bpa by bio-layer interferometry (BLI).

catalytic radical coupling, offer a promising solution. To rigorously evaluate the bioorthogonality and biocompatibility of our photocatalytic labeling in sensitive neuronal environments, we introduced benzophenone groups into primary neurons using SulfoNHS-BP **5**, followed by brief blue LED irradiation to induce ketyl radical coupling with Biotin-BP **6** (Figure 3D). Confocal microscopy revealed specific labeling, characterized by a significant increase in biotinylated signals that robustly colocalized with MAP-2, a key marker of neuronal integrity. This precise spatial overlap demonstrates the method's high selectivity within complex cellular architecture. The labeling process maintained excellent biocompatibility, as quantitatively confirmed by MTT assays showing 84% ± 2% cell viability under standard photocatalytic conditions. Control experiments omitting individual components ([Ru], VcH, or Biotin-BP **6**) confirmed negligible toxicity, and viability remained high across a range of irradiation times and catalyst concentrations, underscoring the method's robustness (Figure S26).[25] While tissue debris and NHS ester-mediated disruptions can introduce minor background, our photocatalytic method maintains exceptional specificity and biocompatibility. These results establish its utility as a true bioorthogonal labeling strategy, even in the most sensitive primary neuronal systems.

https://doi.org/10.1021/jacs.5c18652
J. Am. Chem. Soc. 2025, 147, 45774−45784

Photocatalytic Benzophenone Coupling for Site-Specific Protein Modification by Genetic Code Engineering with Unnatural Amino Acid Bpa. Site-specific protein modification is crucial for enhancing the homogeneity of protein products.[26] To achieve site-specific modification, we genetically incorporated a benzophenone moiety (Bpa) into the solvent-exposed residue N136 of Bcl-X_L using genetic code expansion techniques (Figure 4A).[27] Upon incubation with a small molecule probe Biotin-BP **6** under blue light irradiation, we observed efficient and light-dependent labeling of Bcl-X_L-N136Bpa. Control experiments confirmed the specificity of the reaction, as no labeling occurred in the absence of light or the benzophenone group. LC-MS/MS analysis confirmed the site-specific incorporation of Bpa at residue N136 of Bcl-X_L, demonstrating the precision of the genetic code expansion strategy. Moreover, through photocatalytic ketyl radical reactions, only Bpa at this single site was selectively converted to the pinacol-conjugated biotin, while the biotin modification at other sites was not detected. Remarkably, the method achieved single site-selective labeling of Bcl-X_L-N136Bpa even in complex mixtures containing other proteins and cell lysates, highlighting its high efficiency and excellent orthogonality (Figure S27A−F). Unlike traditional UV-activated diradical mechanisms that enable nonspecific photo-cross-linking, our visible-light-induced diaryl ketyl radical catalysis achieves precise site-specific labeling on Bcl-Bpa. This specificity matches labeling accuracy observed on wild-type Bcl-X_L (Figure 4A, S28).

The photocatalytic ketyl radical coupling reaction is compatible with various imaging groups, such as coumarin, fluorescein, and TAMRA, enabling diverse site-specific imaging applications. The reaction's versatility is further demonstrated by its compatibility with various enrichment handles, including alkyne, dibenzoazacyclooctyne (DBCO), and desthiobiotin, which can be used for affinity purification and other downstream enrichment applications (Figure 4B).[28] The reaction efficiently proceeds at low temperatures (4 °C), making it suitable for temperature-sensitive proteins and reducing the risk of protein denaturation (Figure S27G). Additionally, we successfully applied this Bpa labeling strategy to other protein classes, including fluorescent protein (mCherry) with 9Bpa and nanobody 7D12 with 76Bpa, both of which were site-specifically labeled at solvent-exposed surfaces (Figure S29). These experiments have illustrated the reaction's excellent compatibility with different reporter groups, reaction conditions, and protein types.

To demonstrate the applicability of this site-specific radical coupling strategy for live cell modification, we employed the nanobody 7D12, a high-affinity EGFR binder.[29] This nanobody was genetically engineered to incorporate a benzophenone moiety (Bpa) at residue K76, a site distant from its EGFR-binding domain, using genetic code expansion techniques (Figure S30).[30] HEK293T cells expressing EGFR-EGFP were treated with the modified nanobody 7D12−76Bpa, enabling specific binding to EGFR. Subsequent photocatalytic coupling with Biotin-BP **6** efficiently labeled the modified nanobody on live-cell membrane, as confirmed by confocal microscopy (Figure 4C). Control experiments with wild-type 7D12 demonstrated the specificity of the reaction, with minimal background fluorescence. Overlay images and line profile analysis confirmed the colocalization of the labeling signal with EGFR-EGFP expression, indicating site-specific modification of the 7D12 nanobody on live-cell membranes (Figure S31−S32).[31] Unlike UV-induced controls that showed nonspecific labeling, our mild photocatalytic labeling demonstrated superior spatial specificity by minimizing off-target signal (Figure 4C).

Photocatalytic Benzophenone Coupling to Explore Protein−Protein Interactions at Atomic-Level Precision. Protein cross-linking is essential for studying protein−protein interactions. Among these, cross-linking at particular amino acid residues with site-specificity enables precise analysis of protein complex structures.[32] Traditional protein cross-linking methods often rely on natural amino acids like cysteines, which can form unstable cystine cross-links (Figure 5A). While incorporating unnatural amino acids (UAAs) bearing bioorthogonal handles can enable irreversible linkages to probe protein−protein interactions, the requirement for two different sets of UAAs can increase experimental complexity.[33] Our ketyl radical−radical coupling approach, using a single set of UAAs, offers a simpler and more efficient method for site-specific and stable protein cross-linking.[27]

To validate our approach, we selected PyrI4, a homodimeric protein that catalyzes the Diels−Alder reaction.[34] We strategically incorporated Bpa at position 138 of PyrI4, a residue located within the protein−protein interface but not essential for its function (PDB entry 5BTU). The modified PyrI4 complex was subjected to standard photocatalytic conditions for 10 min. SDS-PAGE analysis revealed the formation of a higher molecular weight band corresponding to the cross-linked PyrI4−138Bpa dimer, while the wild-type protein remained monomeric (Figure 5B). Control experiments confirmed that protein cross-linking was dependent on the presence of both the photocatalyst and light irradiation. LC-MS/MS analysis unequivocally demonstrated site-specific protein cross-linking, a direct consequence of the chemical transformation of benzophenone to pinacol through ketyl radical−radical coupling (Figure S33).

To expand the utility of our method, we investigated its potential for studying heteromeric protein−protein interactions. We selected Trx/PAPS and Bcl-X_L/Bid, two well-characterized protein complexes involved in redox homeostasis and apoptosis, respectively (PDB entries 2O8V and 4QVE). We strategically incorporated Bpa at interface residues—Q62 on Trx, Y191 on PAPS, V126 on Bcl-X_L, and I83 on Bid—to facilitate site-specific cross-linking upon photocatalytic activation. Electrophoresis confirmed the formation of covalent Trx-PAPS and covalent Bcl-X_L-Bid complexes, respectively. Control experiments underscored the specificity and efficiency of the reaction, highlighting its potential to elucidate complex protein−protein interactions at atomic-level precision. Tandem mass spectrometry confirmed the formation of a pinacol linkage between the Bpa residues, supporting the proposed cross-linking mechanism via ketyl radical coupling (Figure 5B-D, Figure S34). These experiments demonstrate the successful site-specific cross-linking of heteromeric protein−protein pairs using photocatalytic ketyl radical coupling. To ensure the site-specificity of our cross-linking strategy relying on proximity for efficient cross-linking,[31] we performed control experiments. By introducing Bpa at a distant site on Bcl-X_L (A171) or disrupting the protein−protein interaction through heat treatment (Figure 5E, Figure S35A), we demonstrated that cross-linking was inhibited. Additionally, crossover experiments between noninteracting proteins (PyrI4−138Bpa and Bid-83Bpa) unequivocally confirmed the critical role of

https://doi.org/10.1021/jacs.5c18652
J. Am. Chem. Soc. 2025, 147, 45774−45784

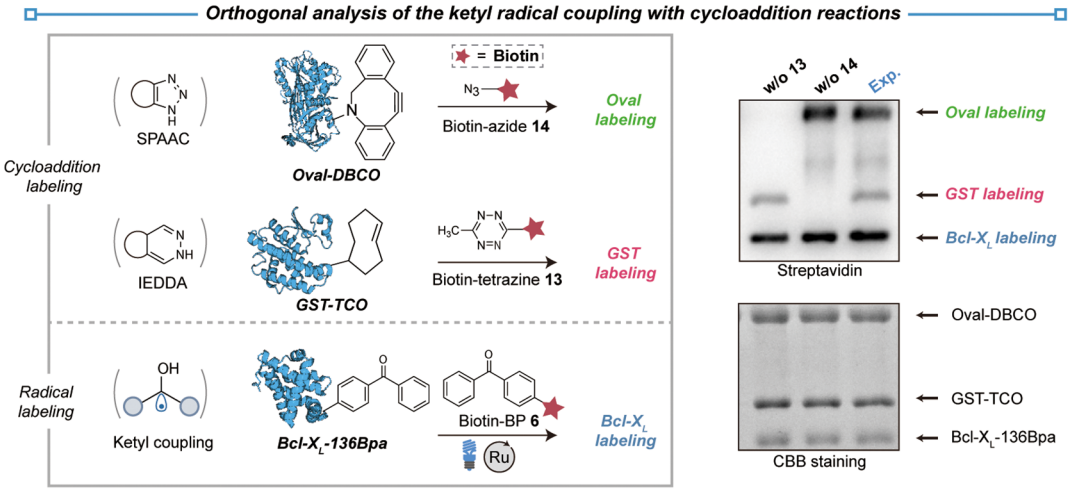

Figure 6. Orthogonal analysis of the ketyl radical coupling with cycloaddition reactions. Bcl-X_L-136Bpa (10 μM), GST-TCO (10 μM), and Oval-DBCO (10 μM) reacted with Biotin-BP **6** (100 μM), Biotin-tetrazine **13** (100 μM), and Biotin-azide **14** (100 μM) under standard photocatalytic conditions (10 μM $Ru(bpy)_3Cl_2$, 20 mM VcH, 468 nm light irradiation for 10 min). The results were analyzed by Western blots.

proximity, further validating the specificity of our photocatalytic ketyl radical coupling approach (Figure S35B).

A concern regarding the potential steric hindrance introduced by the bulky benzophenone moiety arose. To ensure that Bpa incorporation did not disrupt protein structure, function, or protein−protein interactions, we performed molecular dynamics simulations and biophysical experiments. Our simulations revealed that incorporating Bpa at residue 136 of Bcl-X_L had a minimal impact on the protein's helical structure, bound conformation, and binding affinity to the Bid peptide compared to the wild-type complex (Figure 5F, Figure S35C−D).[35] Bio-Layer Interferometry (BLI) further confirmed the robust binding affinity between Bcl-X_L-126Bpa and Bid-83Bpa, with a dissociation constant (K_D) of 1.77 μM (Figure 5G). These results demonstrate that our photocatalytic ketyl radical coupling strategy enables precise protein modification while preserving native protein structure and function, highlighting its atomic-level precision.

Orthogonal Analysis of the Ketyl Radical Coupling with Cycloaddition Reactions. A significant feature of this new bioorthogonal reaction is its excellent compatibility with commonly used bioorthogonal manifolds. Leveraging its unique radical mechanism, we hypothesized that photocatalytic ketyl radical coupling could be combined with other widely used bioorthogonal techniques like strain-promoted alkyne−azide cycloaddition (SPAAC) and inverse-electron-demand Diels−Alder (IEDDA) reactions for multiplex labeling.[36] To demonstrate this, we modified glutathione S-transferase (GST) and ovalbumin (Oval) with different bioorthogonal tags: trans-cyclooctene (TCO) for GST and dibenzoazacyclooctyne (DBCO) for ovalbumin, using NHS ester chemistry (Figure 6). Next, we incubated a mixture of these proteins (10 μM each): GST-TCO, Oval-DBCO, and Bcl-X_L-136Bpa, with a probe mixture (100 μM each): Biotin-BP **6**, Biotin-tetrazine **13**, and Biotin-azide **14** under photocatalytic conditions.

Western blot analysis revealed efficient labeling of all three proteins with their corresponding biotinylated probes (lane 3). This result demonstrates the orthogonal nature of the three reactions, as they proceed independently under the specified conditions. Control experiments, omitting either biotin-azide **14** or biotin-tetrazine **13**, confirmed the orthogonality of the reactions, with no background coupling observed for Oval or GST proteins, respectively (lanes 1 and 2). These findings demonstrate the orthogonal reactivity of photocatalytic radical coupling with SPAAC and IEDDA reactions. This orthogonality enables the seamless integration of these reactions, opening new possibilities for versatile and multiplexed protein applications.

CONCLUSIONS

In conclusion, we have developed a novel bioorthogonal strategy for protein modification and cross-linking based on the photocatalytic coupling of stabilized diaryl ketyl radicals. Unlike traditional methods employing light-induced excitation of benzophenones to generate highly reactive triplet diradicals, our approach utilizes visible light photocatalysis to generate stabilized ketyl radicals, enabling selective modification and cross-linking in complex biological environments. By leveraging the unique balance of stability and reactivity inherent to these stabilized ketyl radicals, we have demonstrated their efficacy for modifying proteins in live cells, including sensitive primary neurons, and for probing protein−protein interactions, providing atomic-level insights into systems such as PyrI4 and the Bcl-X_L/Bid complex. This photocatalytic ketyl radical coupling strategy provides a valuable tool for investigating biological processes with high spatiotemporal control and enhanced selectivity compared to existing benzophenone-based methods. We anticipate that this method will find broad applications in chemical biology, drug discovery, and potentially *in vivo* protein modifications.

ASSOCIATED CONTENT

Supporting Information

The Supporting Information is available free of charge at https://pubs.acs.org/doi/10.1021/jacs.5c18652.

Complete mechanistic experiments, optimization tables, experimental methods, and additional experimental data (PDF)

AUTHOR INFORMATION

Corresponding Authors

Renxiao Wang − *Department of Medicinal Chemistry, School of Pharmacy, Fudan University, Shanghai 201203, China;*

https://doi.org/10.1021/jacs.5c18652
J. Am. Chem. Soc. 2025, 147, 45774−45784

orcid.org/0000-0003-0485-0259; Email: wangrx@fudan.edu.cn

Yaoyang Zhang − *Interdisciplinary Research Center on Biology and Chemistry, Shanghai Institute of Organic Chemistry, Chinese Academy of Sciences, Shanghai 201210, China; Shanghai Key Laboratory of Aging Studies, Shanghai 201210, China;* orcid.org/0000-0001-5363-9834; Email: zyy@sioc.ac.cn

Yiyun Chen − *State Key Laboratory of Chemical Biology, Shanghai Institute of Organic Chemistry, University of Chinese Academy of Sciences, Chinese Academy of Sciences, Shanghai 200032, China; School of Physical Science and Technology, ShanghaiTech University, Shanghai 201210, China; School of Chemistry and Material Sciences, Hangzhou Institute for Advanced Study, University of Chinese Academy of Sciences, Hangzhou 310024, China;* orcid.org/0000-0003-0916-0994; Email: yiyunchen@sioc.ac.cn

Authors

Jiawei Tan − *State Key Laboratory of Chemical Biology, Shanghai Institute of Organic Chemistry, University of Chinese Academy of Sciences, Chinese Academy of Sciences, Shanghai 200032, China*

Kejia Hao − *State Key Laboratory of Chemical Biology, Shanghai Institute of Organic Chemistry, University of Chinese Academy of Sciences, Chinese Academy of Sciences, Shanghai 200032, China*

Yi Yuan − *Interdisciplinary Research Center on Biology and Chemistry, Shanghai Institute of Organic Chemistry, Chinese Academy of Sciences, Shanghai 201210, China; University of Chinese Academy of Sciences, Beijing 100049, China*

Shasha Xie − *State Key Laboratory of Chemical Biology, Shanghai Institute of Organic Chemistry, University of Chinese Academy of Sciences, Chinese Academy of Sciences, Shanghai 200032, China*

Li Qi − *State Key Laboratory of Chemical Biology, Shanghai Institute of Organic Chemistry, University of Chinese Academy of Sciences, Chinese Academy of Sciences, Shanghai 200032, China*

Qiaoling Che − *State Key Laboratory of Chemical Biology, Shanghai Institute of Organic Chemistry, University of Chinese Academy of Sciences, Chinese Academy of Sciences, Shanghai 200032, China; School of Physical Science and Technology, ShanghaiTech University, Shanghai 201210, China*

Yan Li − *Department of Medicinal Chemistry, School of Pharmacy, Fudan University, Shanghai 201203, China;* orcid.org/0000-0002-8259-2470

Complete contact information is available at: https://pubs.acs.org/10.1021/jacs.5c18652

Author Contributions

#J.T., K.H., Y.Y., S.X., L.Q., and Q.C. contributed equally to this work.

Notes

The authors declare no competing financial interest.

■ ACKNOWLEDGMENTS

This research was supported by the National Natural Science Foundation of China (grants 22337005, 22277133), the Strategic Priority Research Program of the Chinese Academy of Sciences (XDB1060000), the Youth Innovation Promotion Association CAS (2023266), Shanghai Oriental Talent Leadership Program, Shanghai Municipal Science and Technology Major Project, the Shanghai Basic Research Pioneer Project, and the Shanghai Key Laboratory of Aging Studies (19DZ2260400). We thank Ms. Chen Su and Dr. Chao Peng of the Mass Spectrometry System at the National Facility for Protein Science in Shanghai (NFPS) for their contributions to MS sample preparation, data collection, and analysis. We also thank Ms. Yang Liu and Prof. Kaiwen He for providing the primary neuron samples.

■ REFERENCES

(1) (a) Renaud, P.; Sibi, M. P., Eds. *Radicals in Organic Synthesis*; Wiley-VCH, 2001. (b) Yan, M.; Lo, J. C.; Edwards, J. T.; Baran, P. S. Radicals: Reactive Intermediates with Translational Potential. *J. Am. Chem. Soc.* **2016**, *138*, 12692−12714.

(2) (a) Yorimitsu, H.; Shinokubo, H.; Oshima, K. Synthetic radical reactions in aqueous media. *Synlett* **2002**, *2002*, 674−686. (b) Chen, X.; Josephson, B.; Davis, B. G. Carbon-Centered Radicals in Protein Manipulation. *ACS. Cent Sci.* **2023**, *9*, 614−638. (c) Huang, H.; Zhang, G.; Gong, L.; Zhang, S.; Chen, Y. Visible-Light-Induced Chemoselective Deboronative Alkynylation under Biomolecule-Compatible Conditions. *J. Am. Chem. Soc.* **2014**, *136*, 2280−2283. (d) Wright, T. H.; Bower, B. J.; Chalker, J. M.; Bernardes, G. J. L.; Wiewiora, R.; Ng, W.-L.; Raj, R.; Faulkner, S.; Vallée, M. R. J.; Phanumartwiwath, A.; Coleman, O. D.; Thézénas, M.-L.; Khan, M.; Galan, S. R. G.; Lercher, L.; Schombs, M. W.; Gerstberger, S.; Palm-Espling, M. E.; Baldwin, A. J.; Kessler, B. M.; Claridge, T. D. W.; Mohammed, S.; Davis, B. G. Posttranslational mutagenesis: A chemical strategy for exploring protein side-chain diversity. *Science* **2016**, *354*, aag1465.

(3) (a) Geri, J. B.; Oakley, J. V.; Reyes-Robles, T.; Wang, T.; McCarver, S. J.; White, C. H.; Rodriguez-Rivera, F. P.; Parker, D. L.; Hett, E. C.; Fadeyi, O. O.; Oslund, R. C.; MacMillan, D. W. C. Microenvironment mapping via Dexter energy transfer on immune cells. *Science* **2020**, *367*, 1091−1097. (b) Liu, W.; Watson, E. E.; Winssinger, N. Photocatalysis in Chemical Biology: Extending the Scope of Optochemical Control and Towards New Frontiers in Semisynthetic Bioconjugates and Biocatalysis. *Helv. Chim. Acta* **2021**, *104*, No. e2100179. (c) Wang, H.; Zhang, Y.; Zeng, K.; Qiang, J.; Cao, Y.; Li, Y.; Fang, Y.; Zhang, Y.; Chen, Y. Selective Mitochondrial Protein Labeling Enabled by Biocompatible Photocatalytic Reactions inside Live Cells. *JACS Au* **2021**, *1*, 1066−1075. (d) Tay, N. E. S.; Ryu, K. A.; Weber, J. L.; Olow, A. K.; Cabanero, D. C.; Reichman, D. R.; Oslund, R. C.; Fadeyi, O. O.; Rovis, T. Targeted activation in localized protein environments via deep red photoredox catalysis. *Nat. Chem.* **2023**, *15*, 101−109. (e) Lin, Z.; Schaefer, K.; Lui, I.; Yao, Z.; Fossati, A.; Swaney, D. L.; Palar, A.; Sali, A.; Wells, J. A. Multiscale photocatalytic proximity labeling reveals cell surface neighbors on and between cells. *Science* **2024**, *385*, No. eadl5763. (f) Zhang, Y.; Liu, Z.; Zhou, N.; Guo, F.; Guo, H.; Chen, X.; Qin, S.; Chen, P. R.; Fan, X. In situ lysosomal proteomics enabled by bioorthogonal photocatalytic proximity labelling. *Nat. Catal.* **2025**, *8*, 162−177. (g) Zhang, Y.; Huang, Y.; Che, Q.; Chen, Y. Photocatalytic Aldehyde Allylation for Site-Specific DNA Functionalization. *Chin. J. Chem.* **2025**, *43*, 97−103.

(4) (a) Hu, C.; Chen, Y. Biomolecule-compatible chemical bond-formation and bond-cleavage reactions induced by visible light. *Tetrahedron Lett.* **2015**, *56*, 884−888. (b) Mascarenas, J. L.; Mato, M.; Fernandez-Gonzalez, X.; D'Avino, C.; Tomas-Gamasa, M. Bioorthogonal Synthetic Chemistry Enabled by Visible-Light Photocatalysis. *Angew. Chem., Int. Ed.* **2024**, *63*, No. e202413506. (c) Teders, M.; Henkel, C.; Anhauser, L.; Strieth-Kalthoff, F.; Gomez-Suarez, A.; Kleinmans, R.; Kahnt, A.; Rentmeister, A.; Guldi, D.; Glorius, F. The energy-transfer-enabled biocompatible disulfide-ene reaction. *Nat. Chem.* **2018**, *10*, 981−988. (d) De Geyter, E.; Antonatou, E.; Kalaitzakis, D.; Smolen, S.; Iyer, A.; Tack, L.; Ongenae, E.; Vassilikogiannakis, G.; Madder, A. 5-Hydroxy-pyrrolone based

building blocks as maleimide alternatives for protein bioconjugation and single-site multi-functionalization. *Chem. Sci.* **2021**, *12*, 5246−5252. (e) Zhang, Y.; Tan, J.; Chen, Y. Visible-Light-Induced Proteins Labeling in Live Cells with Aryl Azides. *Chem. Commun.* **2023**, *59*, 2413−2420.

(5) (a) Biegasiewicz, K. F.; Cooper, S. J.; Gao, X.; Oblinsky, D. G.; Kim, J. B.; Garfinkle, S. E.; Joyce, L. A.; Sandoval, B. A.; Scholes, G. D.; Hyster, T. K. Photoexcitation of flavoenzymes enables a stereoselective radical cyclization. *Science* **2019**, *364*, 1166−1169. (b) Josephson, B.; Fehl, C.; Isenegger, P. G.; Nadal, S.; Wright, T. H.; Poh, A. W. J.; Bower, B. J.; Giltrap, A. M.; Chen, L.; Batchelor-McAuley, C.; Roper, G.; Arisa, O.; Sap, J. B. I.; Kawamura, A.; Baldwin, A. J.; Mohammed, S.; Compton, R. G.; Gouverneur, V.; Davis, B. G. Light-driven post-translational installation of reactive protein side chains. *Nature* **2020**, *585*, 530−537. (c) Wang, T.-C.; Mai, B. K.; Zhang, Z.; Bo, Z.; Li, J.; Liu, P.; Yang, Y. Stereoselective amino acid synthesis by photobiocatalytic oxidative coupling. *Nature* **2024**, *629*, 98−104.

(6) (a) Sato, S.; Nakamura, H. Ligand-directed selective protein modification based on local single-electron-transfer catalysis. *Angew. Chem., Int. Ed.* **2013**, *52*, 8681−8684. (b) Oslund, R. C.; Reyes-Robles, T.; White, C. H.; Tomlinson, J. H.; Crotty, K. A.; Bowman, E. P.; Chang, D.; Peterson, V. M.; Li, L.; Frutos, S.; Vila-Perello, M.; Vlerick, D.; Cromie, K.; Perlman, D. H.; Ingale, S.; Hara, S. D. O.; Roberts, L. R.; Piizzi, G.; Hett, E. C.; Hazuda, D. J.; Fadeyi, O. O. Detection of cell-cell interactions via photocatalytic cell tagging. *Nat. Chem. Biol.* **2022**, *18*, 850−858.

(7) (a) Parsaee, F.; Senarathna, M. C.; Kannangara, P. B.; Alexander, S. N.; Arche, P. D. E.; Welin, E. R. Radical philicity and its role in selective organic transformations. *Nat. Rev. Chem.* **2021**, *5*, 486−499. (b) Fancy, D. A.; Kodadek, T. Chemistry for the analysis of protein−protein interactions: Rapid and efficient cross-linking triggered by long wavelength light. *Proc. Natl. Acad. Sci. U. S. A.* **1999**, *96*, 6020−6024. (c) Li, B. X.; Kim, D. K.; Bloom, S.; Huang, R. Y.; Qiao, J. X.; Ewing, W. R.; Oblinsky, D. G.; Scholes, G. D.; MacMillan, D. W. C. Site-selective tyrosine bioconjugation via photoredox catalysis for native-to-bioorthogonal protein transformation. *Nat. Chem.* **2021**, *13*, 902−908.

(8) Dorman, G.; Nakamura, H.; Pulsipher, A.; Prestwich, G. D. The Life of Pi Star: Exploring the Exciting and Forbidden Worlds of the Benzophenone Photophore. *Chem. Rev.* **2016**, *116*, 15284−15398.

(9) (a) Fischer, H. The Persistent Radical Effect: A Principle for Selective Radical Reactions and Living Radical Polymerizations. *Chem. Rev.* **2001**, *101*, 3581−3610. (b) Goodwin, M. J.; Dickenson, J. C.; Ripak, A.; Deetz, A. M.; McCarthy, J. S.; Meyer, G. J.; Troian-Gautier, L. Factors that Impact Photochemical Cage Escape Yields. *Chem. Rev.* **2024**, *124*, 7379−7464.

(10) (a) Sletten, E. M.; Bertozzi, C. R. Bioorthogonal Chemistry: Fishing for Selectivity in a Sea of Functionality. *Angew. Chem., Int. Ed.* **2009**, *48*, 6974−6998. (b) Agard, N. J.; Prescher, J. A.; Bertozzi, C. R. A Strain-Promoted [3 + 2] Azide−Alkyne Cycloaddition for Covalent Modification of Biomolecules in Living Systems. *J. Am. Chem. Soc.* **2004**, *126*, 15046−15047. (c) Blackman, M. L.; Royzen, M.; Fox, J. M. Tetrazine Ligation: Fast Bioconjugation Based on Inverse-Electron-Demand Diels−Alder Reactivity. *J. Am. Chem. Soc.* **2008**, *130*, 13518−13519. (d) Wang, H.; Li, W.; Zeng, K.; Wu, Y.; Zhang, Y.; Xu, T.; Chen, Y. Photocatalysis Enables Visible Light Uncaging of Bioactive Molecules in Live Cells. *Angew. Chem., Int. Ed.* **2019**, *58*, 561−565.

(11) (a) Smith, M. B.; March, J. *March's Advanced Organic Chemistry*; Wiley: 2006. (b) Garwood, J. J. A.; Chen, A. D.; Nagib, D. A. RadicalPolarity. *J. Am. Chem. Soc.* **2024**, *146*, 28034−28059.

(12) (a) Nakajima, M.; Fava, E.; Loescher, S.; Jiang, Z.; Rueping, M. Photoredox-Catalyzed Reductive Coupling of Aldehydes, Ketones, and Imines with Visible Light. *Angew. Chem., Int. Ed.* **2015**, *54*, 8828−32. (b) Qi, L.; Chen, Y. Polarity-Reversed Allylations of Aldehydes, Ketones, and Imines Enabled by Hantzsch Ester in Photoredox Catalysis. *Angew. Chem., Int. Ed.* **2016**, *55*, 13312−13315. (c) Zhang, J.; Liu, D.; Liu, S.; Ge, Y.; Lan, Y.; Chen, Y. Visible-Light-Induced Alkoxyl Radicals Enable α-C(sp3)-H Bond Allylation. *iScience* **2020**, *23*, 100755.

(13) Beckett, A.; Porter, G. Primary photochemical processes in aromatic molecules. Part 9. —Photochemistry of benzophenone in solution. *Trans. Faraday Soc.* **1963**, *59*, 2038−2050.

(14) Dormán, G.; Nakamura, H.; Pulsipher, A.; Prestwich, G. D. The Life of Pi Star: Exploring the Exciting and Forbidden Worlds of the Benzophenone Photophore. *Chem. Rev.* **2016**, *116*, 15284−15398.

(15) Koniev, O.; Wagner, A. Developments and recent advancements in the field of endogenous amino acid selective bond forming reactions for bioconjugation. *Chem. Soc. Rev.* **2015**, *44*, 5495−5551.

(16) (a) Ji, X.; Khdour, O. M.; Hecht, S. M. Multifunctional Radical Quenchers as Potential Therapeutic Agents for the Treatment of Mitochondrial Dysfunction. *Future Med. Chem.* **2019**, *11*, 1605−1624. (b) Strehmel, V. RadicalsinIonicLiquids. *ChemPhysChem* **2012**, *13*, 1649−1663.

(17) Speckmeier, E.; Zeitler, K. Desyl and Phenacyl as Versatile, Photocatalytically Cleavable Protecting Groups: A Classic Approach in a Different (Visible) Light. *ACS Catal.* **2017**, *7*, 6821−6826.

(18) Kramarenko, G. G.; Hummel, S. G.; Martin, S. M.; Buettner, G. R. Ascorbate reacts with singlet oxygen to produce hydrogen peroxide. *Photochem. Photobiol.* **2006**, *82*, 1634−1637.

(19) Strieth-Kalthoff, F.; James, M. J.; Teders, M.; Pitzer, L.; Glorius, F. Energy transfer catalysis mediated by visible light: principles, applications, directions. *Chem. Soc. Rev.* **2018**, *47*, 7190−7202.

(20) Devaraj, N. K. The Future of Bioorthogonal Chemistry. *ACS Cent. Sci.* **2018**, *4*, 952−959.

(21) Encinas, S.; Belmadoui, N.; Climent, M. J.; Gil, S.; Miranda, M. A. Photosensitization of Thymine Nucleobase by Benzophenone Derivatives as Models for Photoinduced DNA Damage: Paterno−Büchi vs Energy and Electron Transfer Processes. *Chem. Res. Toxicol.* **2004**, *17*, 857−862.

(22) (a) Becker, B. F. Towards the physiological function of uric acid. *Free Radical Biol. Med.* **1993**, *14*, 615−631. (b) Roy, I.; Ohulchanskyy, T. Y.; Pudavar, H. E.; Bergey, E. J.; Oseroff, A. R.; Morgan, J.; Dougherty, T. J.; Prasad, P. N. Ceramic-Based Nanoparticles Entrapping Water-Insoluble Photosensitizing Anticancer Drugs: A Novel Drug−Carrier System for Photodynamic Therapy. *J. Am. Chem. Soc.* **2003**, *125*, 7860−7865.

(23) Bullmore, E. T.; Sporns, O. Complex brain networks: graph theoretical analysis of structural and functional systems. *Nat. Rev. Neurosci.* **2009**, *10*, 186−198.

(24) (a) Liu, S.; Lin, C.; Xu, Y.; Luo, H.; Peng, L.; Zeng, X.; Zheng, H.; Chen, P. R.; Zou, P. A far-red hybrid voltage indicator enabled by bioorthogonal engineering of rhodopsin on live neurons. *Nat. Chem.* **2021**, *13*, 472−479. (b) Bessa-Neto, D.; Beliu, G.; Kuhlemann, A.; Pecoraro, V.; Doose, S.; Retailleau, N.; Chevrier, N.; Perrais, D.; Sauer, M.; Choquet, D. Bioorthogonal labeling of transmembrane proteins with non-canonical amino acids unveils masked epitopes in live neurons. *Nat. Commun.* **2021**, *12*, 6715. (c) Arsic, A.; Hagemann, C.; Stajkovic, N.; Schubert, T.; Nikic-Spiegel, I. Minimal genetically encoded tags for fluorescent protein labeling in living neurons. *Nat. Commun.* **2022**, *13*, 314. (d) Zeng, K.; Jiao, Z.; Jiang, Q.; He, R.; Zhang, Y.; Li, W.; Xu, T.; Chen, Y. Genetically Encoded Photocatalysis Enables Spatially Restricted Optochemical Modulation of Neurons in Live Mice. *ACS Cent. Sci.* **2024**, *10*, 163−175.

(25) Johnson, G. V. W.; Jope, R. S. The role of microtubule-associated protein 2 (MAP-2) in neuronal growth, plasticity, and degeneration. *J. Neurosci. Res.* **1992**, *33*, 505−512.

(26) Krall, N.; da Cruz, F. P.; Boutureira, O.; Bernardes, G. J. L. Site-selective protein-modification chemistry for basic biology and drug development. *Nat. Chem.* **2016**, *8*, 103−113.

(27) Ryu, Y.; Schultz, P. G. Efficient incorporation of unnatural amino acids into proteins in Escherichia coli. *Nat. Methods* **2006**, *3*, 263−265.

(28) Parker, C. G.; Pratt, M. R. Click Chemistry in Proteomic Investigations. *Cell* **2020**, *180*, 605−632.

(29) Lang, K.; Davis, L.; Torres-Kolbus, J.; Chou, C.; Deiters, A.; Chin, J. W. Genetically encoded norbornene directs site-specific

https://doi.org/10.1021/jacs.5c18652
J. Am. Chem. Soc. 2025, 147, 45774−45784

cellular protein labelling via a rapid bioorthogonal reaction. *Nat. Chem.* **2012**, *4*, 298−304.
(30) (a) Roovers, R. C.; Laeremans, T.; Huang, L.; De Taeye, S.; Verkleij, A. J.; Revets, H.; de Haard, H. J.; van Bergen en Henegouwen, P. M. P. Efficient inhibition of EGFR signalling and of tumour growth by antagonistic anti-EGFR Nanobodies. *Cancer Immunol. Immunother.* **2007**, *56*, 303−317. (b) Roovers, R. C.; Vosjan, M. J. W. D.; Laeremans, T.; el Khoulati, R.; de Bruin, R. C.G.; Ferguson, K. M.; Verkleij, A. J.; van Dongen, G. A. M. S.; van Bergen en Henegouwen, P. M. P. A biparatopic anti-EGFR nanobody efficiently inhibits solid tumour growth. *Int. J. Cancer* **2011**, *129*, 2013−2024.
(31) Schumacher, D.; Helma, J.; Schneider, A. F. L.; Leonhardt, H.; Hackenberger, C. P. R. Nanobodies: Chemical Functionalization Strategies and Intracellular Applications. *Angew. Chem., Int. Ed.* **2018**, *57*, 2314−2333.
(32) (a) Lang, K.; Chin, J. W. Cellular Incorporation of Unnatural Amino Acids and Bioorthogonal Labeling of Proteins. *Chem. Rev.* **2014**, *114*, 4764−4806. (b) Liu, D.-D.; Ding, W.; Cheng, J.-T.; Wei, Q.; Lin, Y.; Zhu, T.-Y.; Tian, J.; Sun, K.; Zhang, L.; Lu, P.; Yang, F.; Liu, C.; Tang, S.; Yang, B. Characterize direct protein interactions with enrichable, cleavable and latent bioreactive unnatural amino acids. *Nat. Commun.* **2024**, *15*, 5221. (c) Wang, N.; Yang, B.; Fu, C.; Zhu, H.; Zheng, F.; Kobayashi, T.; Liu, J.; Li, S.; Ma, C.; Wang, P. G.; Wang, Q.; Wang, L. Genetically Encoding Fluorosulfate-l-tyrosine To React with Lysine, Histidine, and Tyrosine via SuFEx in Proteins in Vivo. *J. Am. Chem. Soc.* **2018**, *140*, 4995−4999.
(33) Istrate, A.; Geeson, M. B.; Navo, C. D.; Sousa, B. B.; Marques, M. C.; Taylor, R. J.; Journeaux, T.; Oehler, S. R.; Mortensen, M. R.; Deery, M. J.; Bond, A. D.; Corzana, F.; Jiménez-Osés, G.; Bernardes, G. J. L. Platform for Orthogonal N-Cysteine-Specific Protein Modification Enabled by Cyclopropenone Reagents. *J. Am. Chem. Soc.* **2022**, *144*, 10396−10406.
(34) Zheng, Q.; Guo, Y.; Yang, L.; Zhao, Z.; Wu, Z.; Zhang, H.; Liu, J.; Cheng, X.; Wu, J.; Yang, H.; Jiang, H.; Pan, L.; Liu, W. Enzyme-Dependent [4 + 2] Cycloaddition Depends on Lid-like Interaction of the N-Terminal Sequence with the Catalytic Core in PyrI4. *Cell. Chem. Biol.* **2016**, *23*, 352−360.
(35) Case, D. A.; Ben-Shalom, I. Y.; Brozell, S. R.; Cerutti, D. S.; Cheatham, T. E.; Cruzeiro, V. W. D.; Darden, T. A.; Duke, R. E.; Ghoreishi, D.; Gilson, M. K.; Gohlke, H.; Goetz, A. W.; Greene, D.; Harris, R.; Homeyer, N.; Huang, Y. I. S.; Kovalenko, A.; Kurtzman, T.; Lee, T. S.; LeGrand, S.; Li, P.; Lin, C.; Liu, J.; Luchko, T.; Luo, R.; Mermelstein, D. J.; Merz, K. M.; Miao, Y.; Monard, G.; Nguyen, C.; Nguyen, H.; Omelyan, I.; Onufriev, A.; Pan, F.; Qi, R.; Roe, D. R.; Roitberg, A.; Sagui, C.; Schott-Verdugo, S.; Shen, J.; Simmerling, C. L.; Smith, J.; Salomon-Ferrer, R.; Swails, J.; Walker, R. C.; Wang, J.; Wei, H.; Wolf, R. M.; Wu, X.; Xiao, L.; York, D. M.; Kollman, P. A. *AMBER 2018*, University of California, San Francisco, 2018.
(36) (a) Smeenk, M.; Agramunt, J.; Bonger, K. M. Recent developments in bioorthogonal chemistry and the orthogonality within. *Curr. Opin. Chem. Biol.* **2021**, *60*, 79−88. (b) Li, J.; Kong, H.; Huang, L.; Cheng, B.; Qin, K.; Zheng, M.; Yan, Z.; Zhang, Y. Visible Light-Initiated Bioorthogonal Photoclick Cycloaddition. *J. Am. Chem. Soc.* **2018**, *140*, 14542−14546. (c) Markos, A.; Biedermann, M.; Heimgartner, J.; Schmitt, A.; Lang, K.; Wennemers, H. Introducing Azomethine Imines to Chemical Biology: Bioorthogonal Reaction with Isonitriles. *J. Am. Chem. Soc.* **2023**, *145*, 19513−19517.


CAS BIOFINDER DISCOVERY PLATFORM™
BRIDGE BIOLOGY AND CHEMISTRY FOR FASTER ANSWERS
Analyze target relationships, compound effects, and disease pathways
Explore the platform
CAS
A division of the American Chemical Society

https://doi.org/10.1021/jacs.5c18652
J. Am. Chem. Soc. 2025, 147, 45774−45784